PCCP

Accepted Manuscript

ROYAL SOCIETY OF CHEMISTRY

www.rsc.org/pccp

The acidity/basicity of metal-containing ionic liquids: insights from surface analysis and Fukui function

Weihong Wu, Yunxiang Lu,* Hairong Ding, Changjun Peng, and Honglai Liu

Key Laboratory for Advanced Materials and Department of Chemistry, East China University of Science and Technology, Shanghai 200237, China. E-mail: yxlu@ecust.edu.cn

† Electronic supplementary information (ESI) available. See DOI:

Abstract: Metal-containing ionic liquids (ILs) have been recognized as potential solvents, catalysts, catalyst precursors and reagents for many organic processes. In this work, several quantum-chemical parameters, including surface electrostatic potential ($V_{s,max}$ and $V_{s,min}$), the lowest surface average local ionization energy ($\bar{I}_{s,min}$), and the electrostatic potential at the position of an atom (EP_{nuc}), were adopted to understand the acidity/basicity of metal-containing ILs. Chlorometallate-based ILs show a stronger acidity than conventional ILs, because of the increased electron-deficiency of the imidazole ring with the incorporation of metal chloride. For the ILs with the Ag-coordinated cations, the acidity tends to attenuate while the basicity becomes stronger, as compared to traditional ILs. In addition, the regional Fukui function was also used to assess the molecular distribution of the Lewis acidity/basicity of the ILs under study. Overall, the introduction of metals into either the cations or the anions influences the acidity/basicity of ILs to a large degree, which would be beneficial for their certain applications, such as catalysis and extraction. We hope that the results presented here will assist in the development of novel metal-containing ILs with desirable properties.

1. Introduction

Ionic liquids (ILs) have become one of the most rapidly growing research fields in the last decades, due to their remarkable properties such as negligible low vapor pressure at ambient temperatures, high thermal stability at elevated temperatures, and tunable characters by suitable selection of the cations and anions.[1-4] Many new families and generations of ILs with specific and targeted properties, e.g. multi-functional ILs, bio ILs, chiral ILs, amphiphile ILs, etc., were designed and synthesized.[5,6]

To facilitate the development of a promising IL for a particular use, it is of great importance to obtain accurate knowledge of physicochemical properties of ILs, including their rationalization at a molecular level. In recent years, several experimental studies have been conducted to determine the acidity/basicity of ILs, which is very useful for improving the efficiency of many IL-based processes. For example, the Kamlet-Taft solvatochromic parameters and the hydrogen-bonding acidity/basicity were previously reported for a number of imidazolium and pyridinium-based ILs.[7,8] The acidity and basicity of ILs were also theoretically studied by correlating the experimental values with different computational descriptors.[9-12] In 2013, two complementary models of Lewis molecular acidity (the excess electronic chemical potential and the local charge capacity) were introduced and tested in a series of ILs.[12] Regional electrophilic and nucleophilic Fukui functions were then proposed to efficiently highlight the Lewis acidic/basic distributions of several imidazolium-based ILs.[13] Very recently, Xing and co-workers have demonstrated that the basicity of ILs can be enhanced by tuning the cation-anion interaction strength.[14,15]

Metal-containing ILs, which have many obvious advantages over traditional ILs in such wide applications as Lewis acid catalysts, magnetic fluids, and components in electrochemical deposition process or thermochromic materials, are under active investigation.[16-18] The most common examples are ILs with halometallate anions or metal-coordinated cations.[19-24] Recently, the acidity and basicity of halometallate-based ILs have been examined via X-ray photoelectron spectroscopy.[25] Estager et al. then overviewed halometallate ILs and pointed out that the acidity of these ILs arises from the anion that contains a Lewis acidic center.[26] However, several fundamental questions remain largely elusive to date, for example, why are chlorometallate ILs better Lewis acidic catalysts than conventional ILs? What is the difference

between metal-containing ILs and conventional ILs regarding the acid-base property? Can the order of the acidity/basicity of metal-containing ILs be predicted rationally?

In this work, the nature of the acidity/basicity of metal-containing ILs was studied through a quantitative electrostatic and electronic analysis of molecular surface. Two intrinsic properties of ILs, the maximum surface electrostatic potential ($V_{s,max}$) and the electrostatic potential at the position of an atom (EP_{nuc}), were employed to describe the acidity of a region and an atom, respectively. The minimum surface electrostatic potential ($V_{s,min}$) and the lowest average local ionization energy on the surface ($\bar{I}_{s,min}$) were adopted to understand the basicity of ILs at the electronic level. In addition, the Fukui function, a key quantity that projects the molecular property onto regions of model ion pairs, was also applied to assess the molecular distribution of the Lewis acidicity/basicity of ILs.

2. Theoretical methods

The geometries of the ion pairs for the studied ILs were fully optimized by means of the hybrid B3LYP functional,[27,28] which has been commonly used in the study of cation-anion interactions in ILs.[29-33] The Stuttgart-Cologne multiconfiguration Dirac-Hartree-Fock (MCDHF) adjusted effective core potential (ECP) basis set aug-cc-pVDZ-PP,[34] attained from the EMSL Basis Set Exchange, was employed for I (28 core electrons), Zn (10 core electrons), Ag (28 core electrons) and Hg (60 core electrons), while for the remaining atoms the Dunning's correlation-consistent basis set aug-cc-pVDZ was applied.[35] Very recently, we have successfully utilized the B3LYP/aug-cc-pVDZ(-PP) method to study the structures and electronic properties of halogenated ILs and transition metal-containing ILs.[36,37] All the optimized structures were confirmed to be minima on the potential energy surface via vibrational frequency analysis at the same level of theory. All of these computations were carried out with the help of Gaussian 09 suite of programs.[38] The natural bond orbital (NBO)[39] and Merz-Kollman (MK)[40] atomic charges were evaluated with B3LYP/aug-cc-pVDZ(-PP) for the ion pairs. Although the charges obtained by the two schemes are generally different in magnitude, the conclusions drawn are not affected appreciably.

Cation-anion interaction energies of the ILs were calculated according to eq 1 and were counterpoise-corrected with the procedure of Boys and Bernardi to account for the basis set

superposition error (BSSE):[41]

$$\Delta E_{\mathrm{IL}}\left(\mathrm{kcal/mol}\right) = 627.51\left[E_{AX}(\mathrm{au}) - E_{A^+}(\mathrm{au}) - E_{X^-}(\mathrm{au})\right] \quad (1)$$

where ΔE_{IL} is the cation-anion interaction energy of the ion pair, and E_{AX}, E_{A^+}, and E_{X^-} are the BSSE-corrected energy of the ion pair and the energy of the isolated cation and anion, respectively. Single-point energy calculations were also undertaken at the level of B3LYP/aug-cc-pVTZ(-PP) using the B3LYP/aug-cc-pVDZ(-PP)-optimized structures. As shown in Table 1, the interaction energies of the ion pair calculated with B3LYP/aug-cc-pVTZ(-PP) are somewhat similar to those of B3LYP/aug-cc-pVDZ(-PP).

The electrostatic potential at the position of an atom (EP_{nuc}), neglecting the charge of the atom itself, was computed via a single-point calculation on an optimized geometry using the Gaussian keyword "prop". The surface electrostatic potential ($V_{s,max}$ and $V_{s,min}$) and the surface average local ionization energy ($\bar{I}_{s,min}$) were determined by the Multiwfn 3.3 program,[42] using the B3LYP-optimized geometries, wave functions, and electrostatic potential cube files generated from Gaussian 09. According to the suggestion of Bader et al.,[43] the molecular surface was defined to be the 0.001 a.u. (atomic unit, equals electron/bohr^3) outer contour of its electronic density ρ(r). A visualization tool SurRender was used to obtain the graphs of electrostatic potential and average local ionization energy mapped on the ρ(r) = 0.001 a.u. contour.[44] The regional Fukui function, which is a well-known local descriptor for electron gain and donation, were also calculated with the Multiwfn 3.3 program.

3. Results and discussion

3.1 The acidity/basicity of halometallate ILs

The development of halometallate ILs, e.g. chloroaluminate and chlorozincate ILs, has led to the recognition that ILs are a useful class of functional materials.[19-21,26] Herein, a series of typical halometallate ILs, which are composed of 1-butyl-3-methylimidazolium cation ($[C_4mim]^+$, Scheme 1) and several chlorometallate anions, such as $AlCl_4^-$, $ZnCl_3^-$, $Zn_2Cl_5^-$ and $HgCl_3^-$, were selected. In addition, the conventional IL, [C_4mim][Cl], was also considered for comparison. The most stable geometries of the ion pairs for these ILs are displayed in Fig. 1. For [C_4mim][Cl], the chloride anion is located in the plane of the imidazole ring and close to

the most acidic C^2−H group, whereas the chlorometallate anions tend to reside over the imidazole ring and form two or three H-bonds with the C^2−H moiety and the alkyl chains. As expected, the ion pair of chloride anion exhibits the shortest H(C^2)···Cl interaction distance, thus indicating the strongest C^2−H···Cl H-bond. Consistently, the cation-anion interaction energy of [C_4mim][Cl] is computed much more negative than the ion pairs involving the chlorometallate anions (see Table 1).

The acidity of a molecule is, to some extent, determined by its ability to form electrostatic interactions with basic species. At the microscopic level, $V_{s,max}$ is an effective parameter for interpreting and predicting the acidic region of ILs; the larger magnitude of $V_{s,max}$ implies a stronger acidity or interaction. In addition, the electrostatic potential at the position of an atom K, $EP_{nuc}(K)$ in eq 2, was also evaluated here to describe the acidity around the molecule:

$$EP_{nuc}(K) = \sum_{A \neq k}^{N} \frac{Z_A}{\left|\vec{R}_A - \vec{R}_K\right|} - \int \frac{\rho(\vec{r}\,')}{\left|\vec{r}\,' - \vec{R}_K\right|} d\vec{r}\,' \qquad (2)$$

where Z_A is the nuclear charge of atom A in the molecule at position R_A, and $\left|\vec{R}_A - \vec{R}_K\right|$ is the distance between atom A and atom K. A smaller value of $|EP_{nuc}|$ corresponds to a higher H-bond acidity with a more strongly polarized X−H bond, that is, more charge is pulled away from the H atom, giving rise to a larger Δr that makes $|EP_{nuc}|$ smaller.

Molecular surface properties of the ion pairs for the studied ILs are graphically depicted in Fig. 2, and the corresponding data of $V_{s,max}$ and EP_{nuc} are listed in Table 1. As can be seen, the locations of $V_{s,max}$ for these ILs are all around the H($C^{4/5}$) atom of the cation, in line with the concept that the acidity of ILs frequently comes from the cation. In general, the computed values of $V_{s,max}$ for chlorometallate ILs are larger than that for [C_4mim][Cl]; EP_{nuc} of the three imidazolium H atoms in chlorometallate-based ILs is estimated to be smaller in absolute value compared with [C_4mim][Cl]. These indicate that halometallate ILs exhibit a stronger Lewis acidity than conventional ILs, which has been proved by many experimental studies.[26,45] When a Cl atom in $AlCl_4^-$ was replaced by a Br or I atom, the cation-anion interactions become weaker, and the Lewis acidity increases in the following order: [C_4mim][$AlCl_4$] < [C_4mim][Br-$AlCl_3$]<[C_4mim][I-$AlCl_3$] (cf. Table 1 and Fig. S1), in good agreement with previous experimental findings.[26]

It is well documented the Lewis acidity of chlorometallate ILs is controlled not only by the electrophilicity of the metal but also by the mole fraction of metal chloride used to prepare these ILs.[26] From Table 1, it is clear that the acidity of chlorometallate ILs reduces in the order Al > Zn > Hg, in accordance with the electronegativity trend of the three metals. Additionally, relative to $[C_4mim][ZnCl_3]$, the chlorozincate IL with higher order complex anion ($[C_4mim][Zn_2Cl_5]$) possesses more negative $V_{s,max}$ as well as smaller $|EP_{nuc}|$. Therefore, the Lewis acidity of the ILs becomes stronger with the increase of the mole fraction of metal chloride, consistent with the experimental observations.[9]

Why is the acidity of chlorometallate ILs stronger than traditional ILs? To address this question, the atomic charges and charge transfer properties of the ILs under study were calculated and the results are given in Table 2. Usually, chlorometallate-based ILs were synthesized by direct addition of the required metal chloride MCl_x to $[C_4mim][Cl]$ in appropriate molar ratio and under inert atmosphere. Thus it is speculated that the introduction of metal chloride MCl_x probably contributes to the enhancement of the acidity. For present chlorometallate ILs, charge transfer Q_{CT} indeed occurs from the ion pair unit (C_4mim-Cl), in which the Cl atom is close to the imidazole ring and forms a H-bond with the C^2–H moiety, to the MCl_x unit, as shown in Fig. 3. Moreover, a larger amount of this charge transfer corresponds to a stronger acidity of the ILs (cf. Tables 1 and 2). For example, the magnitude of $Q_{CT}(IP \rightarrow MCl_x)$ for the three aluminate ILs decreases in the following order: $[C_4mim][I\text{-}AlCl_3]$ (484 *me*) > $[C_4mim][Br\text{-}AlCl_3]$ (403 *me*) > $[C_4mim][Cl\text{-}AlCl_3]$ (347 *me*), that is, $AlCl_3$ can attract more electron from $[C_4mim][I]$, leading to the stronger acidity of $[C_4mim][I\text{-}AlCl_3]$. In addition, relative to $[C_4mim][ZnCl_3]$, $Q_{CT}(IP \rightarrow MCl_x)$ appears to be in greater magnitude for $[C_4mim][Zn_2Cl_5]$ that exhibits a stronger acidity. From Table 2, it is also seen that as compared to $[C_4mim][Cl]$, the positive charge on the $H(C^{4/5})$ atom increases and the negative charge on the C^4/C^5 atom also increases in chlorometallate ILs, while the positive charge on the $H(C^2)$ atom in these ILs decreases, thus suggesting charge transfer from $H(C^{4/5})$ to $H(C^2)$, as displayed in Fig. 3. On the basis of these results, the incorporation of metal chloride enhances the electron-deficiency of the imidazole ring, especially on the $H(C^{4/5})$ atom, which gives rise to the stronger acidity of chlorometallate ILs.

Generally, the concept of basicity can be divided into two components: the electrostatic

component and the covalent component. $V_{s,min}$ and $\bar{I}_{s,min}$ can predict the electrostatically reactive ability and the electron-transfer ability of the molecules, respectively. As shown in Fig. 2, the sites of $V_{s,min}$ and $\bar{I}_{s,min}$ are all located at the Cl atom in the anions, irrespective of the anion type (Cl^-, $AlCl_4^-$, $ZnCl_3^-$, $Zn_2Cl_5^-$ and $HgCl_3^-$). Nonetheless, the introduction of metals into the anion affects the magnitude of $V_{s,min}$ and $\bar{I}_{s,min}$ to a large degree. In comparison with [C_4mim][Cl], considerably smaller absolute values of $V_{s,min}$ and much larger $\bar{I}_{s,min}$ are predicted for chlorometallate ILs (see Table 1), which indicates that chlorometallate ILs exhibit a weaker basicity than traditional ILs. This is not surprising, due to the much larger size of chlorometallate anions that results in a more dispersed distribution of the negative charge.

As increasing $ZnCl_2$ content in [C_4mim][$ZnCl_3$], the absolute value of $V_{s,min}$ tends to decrease and the $\bar{I}_{s,min}$ value becomes greater. Consequently, the higher order complex anion leads to less basic ILs, consistent with the experimental results.[9] For the three aluminate ILs, the electrostatically reactive ability increases in the order [C_4mim][$AlCl_4$]＞[C_4mim][Br-$AlCl_3$] ＞[C_4mim][I-$AlCl_3$]; however, the electron-transfer ability follows the reverse trend. This can be explained by the different locations of $\bar{I}_{s,min}$ for these ILs. As is evident from Fig. S1, the $\bar{I}_{s,min}$ site for [C_4mim][Br-$AlCl_3$] and [C_4mim][I-$AlCl_3$] is around the Br atom and the I atom, respectively, rather than the Cl atom in [C_4mim][$AlCl_4$]. It is well known that the electron donating ability of halogen atoms strengthens when going down the periodic table (Cl < Br < I), which gives rise to the observed tendency of $\bar{I}_{s,min}$ for the three ILs. Clearly, both the content of metal halide and the halogen atom in the anion influence the basicity of halometallate ILs.

3.2 The acidity/basicity of the ILs with the Ag-coordinated cations

As compared to halometallate ILs, much less attention has been focused on the ILs involving metals in the cations.[22,23] In this work, three ILs with the cations consisting of silver center coodinated by two *n*-alkylimidazole ligands, i.e. [Ag(mim)$_2$][Tf_2N], [(C_2im)Ag(mim)][Tf_2N], and [(C_4im)Ag(mim)][Tf_2N], were chosen (Scheme 1). In addition, the conventional IL, [C_1mim][Tf_2N], was also taken into account for comparison. Based on the determined crystal structures and our previous calculations,[22,37] the most stable transoid configurations of the ion pairs, in which the anion locates in the front of the cation and forms a strong N···H interaction with the C^2−H group of one imidazole ring, were under investigation, as displayed in Fig. 1. The cation-anion interactions in silver-containing ILs are weaker than

those in [C_1mim][Tf_2N], because of the longer HB distances and less negative interaction energies (see Table 1).

At first, a quantitative analysis of $V_{s,max}$ was performed on these ion pairs. From Fig. 4, it is clear that the location of $V_{s,max}$ in [C_1mim][Tf_2N] is around the H($C^{4/5}$) atom, similar to that in [C_4mim][Cl], whereas the $V_{s,max}$ sites in silver-containing ILs are all around the H($C^{2'}$) atom. Owing to the smaller values of $V_{s,max}$, silver-containing ILs exhibit a weaker acidity than [C_1mim][Tf_2N].

The ability of ILs to act as a H-bond acceptor can be determined by $V_{s,min}$ and $\bar{I}_{s,min}$. As shown in Fig. 4, the sites of $V_{s,min}$ for the studied ILs are all around the O atom in the anion, irrespective of the cation type ($[C_1mim]^+$ and $[(C_nim)Ag(mim)]^+$). Nonetheless, $V_{s,min}$ for silver-containing ILs is predicted to be more negative than that for [C_1mim][Tf_2N], and therefore these ILs behave as stronger H-bond acceptors with respect to conventional ILs. From Fig. 4, it is also seen that the $\bar{I}_{s,min}$ site in [C_1mim][Tf_2N] is located on the anion, while the locations of $\bar{I}_{s,min}$ in the three silver-containing ILs are all around the Ag atom of the cation. It is of great interest to elucidate why the $\bar{I}_{s,min}$ site of these ILs concentrates on the cation. Commonly, the first ionization energy of a molecular is estimated as the difference between the energy of neutral molecular and the energy of the molecular withdrawing an electron which is mostly inclined to escape from the molecular. Here it can be deduced that such electron may come from the HOMO of the ion pairs. As shown in Fig. 5b, the HOMO of [$Ag(mim)_2$][Tf_2N] resides mainly on the cation, rather than the anion, and is composed of the occupied *p* orbitals of the imidazole ring and the *d* obitals of the Ag atom. Therefore, the electron of the Ag atom may leave from the molecular surface more easily, which results in the $\bar{I}_{s,min}$ sites around Ag atom in silver-containing ILs.

3.3 The Fukui function of metal-containing ILs

The Fukui function (FF) shows the distribution of an infinitesimal charge added or removed from a molecule, according to eqs 3 and 4:

$$f^+(r) = \left(\frac{\partial \rho(r)}{\partial N}\right)^+ = \rho_{N+1}(r) - \rho_N(r) \quad (3)$$

$$f^-(r) = \left(\frac{\partial \rho(r)}{\partial N}\right)^- = \rho_N(r) - \rho_{N-1}(r) \quad (4)$$

where $\rho_N(\vec{r})$, $\rho_{N+1}(\vec{r})$, and $\rho_{N-1}(\vec{r})$ are the electron densities of the neutral species (*N*

electrons), its anion (N+1 electrons), and its cation (N−1 electrons), respectively. Electrophilic FF f^+ is the natural distributor of Lewis molecular acidity, and nucleophilic FF f^- is the distributor of Lewis molecular basicity. Here we also can integrate over the corresponding basins $\Omega^{\pm}$ (local area of a molecule), producing the basins FF as follows:

$$N_{\Omega}^{\pm}=\int_{\Omega_k^{\pm}} \rho(\vec{r})\ d\vec{r}=\sum_{k\in\Omega_k^{\pm}} f_k^{\pm} \qquad (5)$$

The basins $\Omega_k^{\pm}$ represent maximum molecular regions of the electrophilic FF (Ω_k^{+}) and nucleophilic FF (Ω_k^{-}), respectively. Thus, the region with the larger N_{Ω}^{+} is the favorable site to accept electron charge, while the region with the greater N_{Ω}^{-} is the location that prefers to donate electron charge.[46] According to the recent work of Cerda-Monje et al,[13] the concept of "normal distribution", "bifunctional distribution" and "borderline distribution" was employed to describe present ILs. Namely, the "normal distribution" indicates that the Lewis molecular acidity (N_{Ω}^{+}) is mainly centered on the cation fragment, and the Lewis molecular basicity (N_{Ω}^{-}) is mostly centered on the anion (for the cation, $N_{\Omega}^{+} >$ 0.9 eV and $N_{\Omega}^{-} <$0.2 eV); the "bifunctional distribution" is used when both the Lewis acidity and basicity are located at the same region of ILs (for the cation, N_{Ω}^{+} > 0.9 ev and $N_{\Omega}^{-} >$ 0.5 eV); the remaining ones belong to the "borderline distribution".

The calculated values of $N_{\Omega}^{\pm}$ for the studied ILs are summarized in Table 3. As can be seen, most of chlorometallate ILs show a normal distribution, that is, the Lewis acidity and basicity is located on the cation and the anion, respectively. However, the ILs involving $HgCl_3^-$ and $Zn_2Cl_5^-$ exhibit a borderline distribution, and therefore some chlorometallate anions can induce electronic polarization on the cation that results in nucleophilic activation in some specific regions. Particularly, for the ILs with the Ag-coordinated cations, the most susceptible site to accept electronic charge as well as the region with the major ability to donate electronic charge are all situated on the cations (bifuncitonal), which can be ascribed to the strengthening nucleophilic ability of the cation with the presence of the Ag atom (cf. Fig. 5).

On the basis of the Lewis acidity/basicity of metal-containing ILs reported herein, some

experimental findings of these ILs can be rationalized at the microscopic level. Recently, Wang and co-workers explored several ILs as efficient catalysts for the glycolysis of poly(ethylene terephthalate) (PET), and they found that halometallate ILs, especially [allyl-mim][$CoCl_3$] and [allyl-mim][$ZnCl_3$], exhibit higher catalytic activity under mild reaction condition, as compared to the traditional catalysts (e.g., $Zn(Ac)_2$) and the conventional IL catalysts (e.g., [C_4mim][Cl]).[47] According to the experimental results, the authors proposed a possible mechanism (see Fig. S2) and raised a reasonable explanation, that is, the higher catalytic activity is attributed to the synergetic effect between the cation and anion of the IL catalyst. As demonstrated in this work, the conventional IL ([C_4mim][Cl]) exhibits a borderline distribution of the Lewis acidity/basicity (for the cation, $N_\Omega^- > 0.2$ eV), and thus the weak nucleophilicity of the cation to some extent hinder it to attack PET. Moreover, the absolute value of EP_{nuc} of the H(C^2) atom in [C_4mim][$ZnCl_3$]) is smaller than that in [C_4mim][Cl] (cf. Table 1), that is, the cation in [C_4mim][$ZnCl_3$] can interact the ester O atom in PET more easily and effectively. In addition, the weaker cation-anion interaction in [C_4mim][$ZnCl_3$] also promotes the $ZnCl_3^-$ anion to interact with the H atom in PET. Overall, the normal distribution of the acidic/basic region, the strong electrostatic interaction with electron, and the weak cation-anion interaction may lead to the better catalytic effect of chlorozincate ILs.

Zhang et al. have previously studied the extraction of aromatic hydrocarbons from aromatic/aliphatic mixtures using chloroaluminate room-temperature ILs as extractants. They pointed out that chloroaluminate ILs can be classified into complexation extraction with a higher capacity and selectivity than traditional ILs with such anions as chloride, bromide, tetrafluoroborate, etc.[48] According to our calculations, the value of $V_{s,max}$ for [C_4mim][$AlCl_4$] is larger than that for [C_4mim][Cl]; the H($C^{4/5}$) atom in [C_4mim][$AlCl_4$] has a smaller absolute value of EP_{nuc} with respect to [C_4mim][Cl]. These indicate that chloroaluminate ILs have stronger acid site to interact with aromatic hydrocarbons with highly delocalized π electron, which may lead to an excellent extraction and separation performance. Additionally, the ILs, [C_4mim][Br-$AlCl_3$] and [C_4mim][I-AlCl3], may also be applied as good extraction solvents, based on our computational results.

4. Conclusions

In this work, $V_{s,max}$ and EP_{nuc} were proposed to describe the acidity of metal-containing ILs, while $V_{s,min}$ and $\bar{I}_{s,min}$ were used to interpret their basicity. The incorporation of metal chloride enhances the electron-deficiency of the imidazole ring, especially on the $H(C^{4/5})$ atom, which leads to the stronger acidity of chlorometallate ILs. Nonetheless, these ILs show a weaker basicity than conventional ILs, because of the dispersed distribution of the negative charge on chlorometallate anions. As compared to traditional ILs, silver-containing ILs exhibit a weaker acidity but behave as stronger H-bond acceptors. In addition, the regional Fukui function was also adopted to investigate the molecular distribution of the Lewis acidity/basicity of the ILs under study. Most of chlorometallate ILs belong to "normal distribution", which seems to be beneficial to the catalytic reaction and extraction, while the ILs with the Ag-coordinated cations can be all considered as "bifunctional distribution". These results not only reveal the acidity and basicity of metal-containing ILs, which is of great importance for a better understanding of the nature of these ILs, but also are highly instructive for the design of new functionalized metal-containing ILs.

Acknowledgements

This work was supported by the National Key Basic Research Program of China (2015CB251401) and the National Natural Science Foundation of China (21473054).

Notes and references

1 R. D. Rogers, *Nature*, 2007, **447**, 917-918.

2 J. Dupont, R. F. de Souza and P. A. Z. Suarez, *Chem. Rev*., 2002, **102**, 3667-3692.

3 A. Rehman and X. Q. Zeng, Acc. Chem. Res., 2012, **45**, 1667-1677.

4 F. Hashim, C. F. Motiwala, S. W. Li, E. Hirt, P. Porubsky, J. Aube, *J. Am. Chem. Soc*., 2013, **135**,9000-9009.

5 H. Olivier-Bourbigou, L. Magna and D. Morvan, *Appl. Catal. A: General*., 2010, **373**, 1-56.

6 M. Smiglak, A. Metlen and R. D. Rogers, *Acc. Chem. Res*., 2007, **40**, 1182-1192.

7 J. M. Lee, S. Ruckes and J. M. Prausnitz, *J. Phys. Chem. B*, 2008, **112**, 1473-1467.

8 J. N. Canongia-Lopes, M. F. C. Gomes, P. Husson, A. A. H. Padua, L. P. N. Rebelo, S.

Sarraute and M. Tariq, *J. Phys. Chem. B*, 2011, **115**, 6088-6099.

9 H. Niedermeyer, C. Ashworth, A. Brandt, T. Welton and P. A. Hunt, *Phys. Chem. Chem. Phys*., 2013, **15**, 11566-11578.

10 C. Yang, X. S. Xue, X. Li and J. P. Cheng, *J. Org. Chem*., 2014, **79**, 4340-4351.

11 J. Palgunadi, S. Y. Hong, J. K. Lee, H. Lee, S. D. Lee, M. Cheong and H. S. Kim, *J. Phys. Chem. B*, 2011, **115**, 1067-1074.

12 R. Contreras, A. Aizman, R. A. Tapia and A. Cerda-Monje, *J. Phys. Chem. B*, 2013, **117**, 1911-1920.

13 A. Cerda-Monje, R. O. Ormazábal-Toledo, C. Cardenas, P. Fuentealba and R. Contreras, *J. Phys. Chem. B*, 2014, **118**, 3696-3701.

14 D. Xu, Q. W. Yang, B. G. Su, Z. B. Bao, Q. L. Ren and H. B. Xing, *J. Phys. Chem. B*, 2014, **118**, 1071-1079.

15 Q. W. Yang, H. B. Xing, Z. B. Bao, B. G. Su, Z. G. Zhang, Y.W. Yang, S. Dai and Q. L. Ren, *J. Phys. Chem. B*, 2014, **118**, 3682-3688.

16 J. P. Hallett and T. Welton, *Chem. Rev*., 2011, **111**, 3508-3576.

17 I. J. B. Lin and C. S.Vasam, *J. Organomet. Chem*., 2005, **690**, 3498-3512.

18 H. Q. N. Gunaratne, T. J. Lotz and K. R. Seddon, *New. J. Chem*., 2010, **34**, 1821-1824.

19 M. Currie, J. Estager, P. Licence, S. Men, P. Nockemann, K. R. Seddon, M. Swadzb and C. Terrade, *Inorg. Chem*., 2013, **52**, 1710-1721.

20 A. P. Abbott, G. Capper, D. L. Davies and R. Rasheed, *Inorg. Chem*., 2004, **43**, 3447-34522.

21 B. Mallick, A. Metlen, M. Nieuwenhuyzen, R. D. Rogers and A. Mudring, *Inorg. Chem*., 2012, **51**, 193-200.

22 N. R. Brooks, S. Schaltin, K. Van Hecke, L. Van Meervelt, J. Fransaerb and K. Binnemans, *Dalton. Trans*., 2012, **41**, 6902-6905.

23 T. V. Hoogerstraete, N. R. Brooks, B. Norberg, J. Wouters, K. Van Hecke, L. Van Meervelt and K. Binnemans, *CrystEngComm*., 2012, **14**, 4902-4911.

24 S. Schaltin, N. R. Brooks, J. Sniekers, D. Depuydt, L. Van Meervelt, K. Binnemans and J. Fransaer, *Phys. Chem. Chem. Phys*., 2013, **15**, 18934-18943.

25 A. W.Taylor, S. Men, C. J. Clarke and P. Licence, *RSC Adv*., 2013, **3**, 9436-9445.

26 J. Estager, J. D. Holbrey and M. S.Kwasny, *Chem. Soc. Rev*., 2014, **43**, 847-866.

27 A. D. Becke, *Phys. Rev. A*, 1988, **38**, 3098-3100.

28 C. Lee, W. Yang and R. G. Parr, *Phys. Rev. B*, 1988, **37**, 785-789.

29 A. M. Fernandes, M. A. A. Rocha, M. G. Freire, I. M. Marrucho, J. A. P. Coutinho and L. M. Stantos, *J. Phys. Chem. B*, 2011, **115**, 4033-4041.

30 K. Dong, Y. Song, X. Liu, W. Cheng, X. Yao and S. J. Zhang, *J. Phys. Chem. B*, 2012, **116**, 1007-1017.

31 P. A. Hunt, B. Kirchner and T. Welton, *Chem. Eur. J.*, 2006, **12**, 6762-6775.

32 H. Niedermeyer, M. A. Ab Rani, P. D. Lickiss, J. P. Hallett, T. Welton, A. J. White and P. A. Hunt, *Phys. Chem. Chem. Phys*., 2010, **12**, 2018-2029.

33 P. A. Hunt, I. R. Gould and B. Kirchner, *Aust. J. Chem*., 2007, **60**, 9-14.

34 K.A. Peterson, D. Figgen, E. Goll, H. Stoll and M. Dolg, *J. Chem. Phys*., 2003, **119** , 11113-11123.

35 R.A. Kendall, T. H. Dunning and R. J. Harrison, *J. Chem. Phys*., 1992, **96**, 6796-6806.

36 W. H. Wu, Y. X. Lu, Y. T. Liu, H. Y. Li, C. J. Peng, H. L. Liu and W. L. Zhu, *J. Phys. Chem. A*, 2014, **118**, 2508-2518.

37 H. Y. Li, Y.X. Lu, W. H. Wu, Y. T. Liu, C. J. Peng, H. L. Liu and W. L. Zhu, *Phys. Chem. Chem. Phys.* 2013, **15**, 4405-4414.

38 M. J. Frisch, G. W. Trucks, H. B. Schlegel, G. E. Scuseria, M. A. Robb, J. R. Cheeseman, G. Scalmani, V. Barone, B. Mennucci, G. A. Petersson, H. Nakatsuji, M. Caricato, X. Li, H. P. Hratchian, A. F. Izmaylov, J. Bloino, G. Zheng, J. L. Sonnenberg, M. Hada, M. Ehara, K. Toyota, R. Fukuda, J. Hasegawa, M. Ishida, T. Nakajima, Y. Honda, O. Kitao, H. Nakai, T. Vreven, J. A. Montgomery, Jr., J. E. Peralta, F. Ogliaro, M. Bearpark, J. J. Heyd, E. Brothers, K. N. Kudin, V. N. Staroverov, R. Kobayashi, J. Normand, K. Raghavachari, A. Rendell, J. C. Burant, S. S. Iyengar, J. Tomasi, M. Cossi, N. Rega, J. M. Millam, M. Klene, J. E. Knox, J. B. Cross, V. Bakken, C. Adamo, J. Jaramillo, R. Gomperts, R. E. Stratmann, O. Yazyev, A. J. Austin, R. Cammi, C. Pomelli, J. W. Ochterski, R. L. Martin, K. Morokuma, V. G. Zakrzewski, G. A. Voth, P. Salvador, J. J. Dannenberg, S. Dapprich, A. D. Daniels, O. Farkas, J. B. Foresman, J. V. Ortiz, J. Cioslowski and D. J. Fox, Gaussian: Wallingford CT, **2009**.

39 A. E. Reed, L. A. Curtiss and F. Weinhold, *Chem. Rev.*, 1988, **88**, 899-926.

40 U. C. Singh and P. A. Kollman, *J. Comput. Chem*. 1984, **5**, 129-145.

41 S. F. Boys and F. Bernardi, *Mol. Phys*., 1970, **19**, 553-556.

42 T. Lu and F. Chen, *J. Comput. Chem*., 2012, **33**, 580-592.

43 R. Bader, M. T. Carroll, J. R. Cheeseman and C. Chang, *J. Am. Chem. Soc*., 1987, **109**, 7968-7979.

44 F. A. Bulat, A. Toro-Labbe, T. Brinck, J. S. Murray and P. Politzer, *J. Mol. Model*. 2010, **16**, 1679-1691.

45 Z. Y. Duan, Y. L. Gu and Y. Q. Deng, *Catal. Commun*. 2006, **7**, 651-656.

46 P. Fuentealba, E. Florez and W. Tiznado, *J. Chem. Theory. Comput*., 2010, **6**, 1470-1478.

47 Q. Wang, X. M. Lu, X. Y. Zhou, M. L. Zhu, H. Y. He and X. P. Zhang, *J. Appl. Polym. Sci*., 2013, **129**, 3574-3581.

48 J. Zhang, C.P. Huang, B. H. Chen, P. J. Ren, Z. G. Lei, *Energy & Fuels*., 2007, **21**, 1724-1730.

Table 1 Cation-anion interaction energies and surface parameters for the studied ILs[a]

ILs	ΔE	$V_{s,max}$	$EP_{nuc}H(C^{2/2'})$	$EP_{nuc}H(C^{4/5})$	$V_{s,min}$	$\bar{I}_{s,min}$
$[C_4mim][Cl]$	-90.77(-90.44)	45.53	-1.0064	-1.0182	-62.29	5.80
$[C_4mim][I\text{-}AlCl_3]$	-68.05(-69.00)	50.93	-1.0025	-0.9971	-35.58	7.12
$[C_4mim][Br\text{-}AlCl_3]$	-69.04(-69.96)	50.59	-1.0027	-0.9982	-36.16	7.89
$[C_4mim][AlCl_4]$	-69.66(-70.71)	50.40	-1.0034	-0.9999	-36.39	8.29
$[C_4mim][ZnCl_3]$	-71.62(-72.84)	49.70	-1.0052	-1.0079	-43.42	7.53
$[C_4mim][Zn_2Cl_5]$	-63.54(-66.92)	50.89	-1.0027	-0.9912	-39.39	7.77
$[C_4mim][HgCl_3]$	-71.96(-73.94)	48.91	-1.0071	-1.0113	-39.08	7.83
$[C_4mim][Tf_2N]$	-75.23(-74.04)	52.60	-0.9940	---	-48.56	9.66
$[Ag(mim)_2][Tf_2N]$	-64.71(-65.16)	46.88	-1.0190	---	-52.78	7.98
$[(C_2mim)Ag(mim)][Tf_2N]$	-64.25(-65.30)	45.14	-1.0220	---	-52.98	7.95
$[(C_4mim)Ag(mim)][Tf_2N]$	-63.82(-64.86)	44.36	-1.0230	---	-53.12	7.94

[a] ΔE, $V_{s,max}$ and $V_{s,min}$ are expressed in kcal/mol, and EP_{nuc} and $\bar{I}_{s,min}$ are given a.u. and eV, respectively. The atomic labels are shown in Scheme 1. The values in parentheses are the interaction energies calculated with B3LYP/aug-cc-pVTZ(-PP).

Table 2 The magnitude of charge transfer from the unit (C_4mim-Cl) to metal chloride [$Q_{CT}(IP \rightarrow MCl_x)$] and NPA charges for the ILs under study[a]

	Q_{CT}	N^1	C^2	$H(C^2)$	N^3	C^4	$H(C^4)$	C^5	$H(C^5)$
$[C_4mim][Cl]$	---	-0.411	0.308	0.289	-0.403	-0.042	0.249	-0.043	0.248
$[C_4mim][I\text{-}AlCl_3]$	-0.484(-0.531)	-0.389	0.331	0.272	-0.390	-0.026	0.254	-0.027	0.254
$[C_4mim][Br\text{-}AlCl_3]$	-0.403(-0.522)	-0.389	0.332	0.273	-0.390	-0.027	0.254	-0.028	0.254
$[C_4mim][AlCl_4]$	-0.347(-0.510)	-0.390	0.332	0.275	-0.390	-0.028	0.254	-0.028	0.275
$[C_4mim][ZnCl_3]$	-0.277(-0.382)	-0.393	0.335	0.283	-0.399	-0.031	0.253	-0.031	0.253
$[C_4mim][Zn_2Cl_5]$	-0.358(-0.430)	-0.387	0.333	0.268	-0.388	-0.019	0.256	-0.022	0.255
$[C_4mim][HgCl_3]$	-0.276(-0.360)	-0.393	0.335	0.284	-0.400	-0.032	0.252	-0.032	0.252

[a] All values are given in a.u. The atomic labels are shown in Scheme 1. The values in parentheses are the amount of charge transfer computed with the MK scheme.

Table 3 Electrophilic (N_{Ω}^{+}) and nucleophilic (N_{Ω}^{-}) FF values over the cations and anions for the studied ILs.

ILs	Cation		Anion		Acidity and bacisity
	N_{Ω}^{+}	N_{Ω}^{-}	N_{Ω}^{+}	N_{Ω}^{-}	Distribution
[C_4mim][Cl]	0.980	0.240	0.020	0.760	borderline
[C_4mim][I-$AlCl_3$]	0.953	0.058	0.047	0.942	normal
[C_4mim][Br-$ZnCl_3$]	0.955	0.116	0.045	0.884	normal
[C_4mim][$AlCl_4$]	0.939	0.190	0.061	0.810	normal
[C_4mim][$ZnCl_3$]	0.958	0.180	0.042	0.820	normal
[C_4mim][Zn_2Cl_5]	0.794	0.156	0.206	0.844	borderline
[C_4mim][$HgCl_3$]	0.560	0.116	0.440	0.884	borderline
[C_4mim][Tf_2N]	0.959	0.208	0.041	0.792	borderline
[$Ag(mim)_2$] [Tf_2N]	0.957	0.584	0.043	0.416	bifunctional
[(C_2mim)Ag(mim)] [Tf_2N]	0.970	0.594	0.030	0.406	bifunctional
[(C_4mim)Ag(mim)] [Tf_2N]	0.984	0.629	0.016	0.371	bifunctional

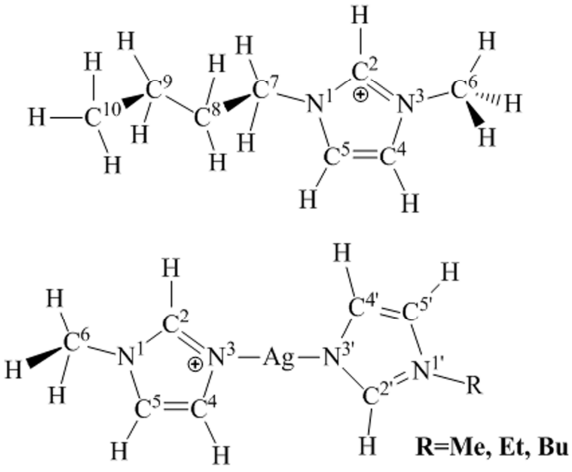

SCHEME 1: The chemical structures of the [C_4mim] and [($C_n$im)Ag(mim)] cations.

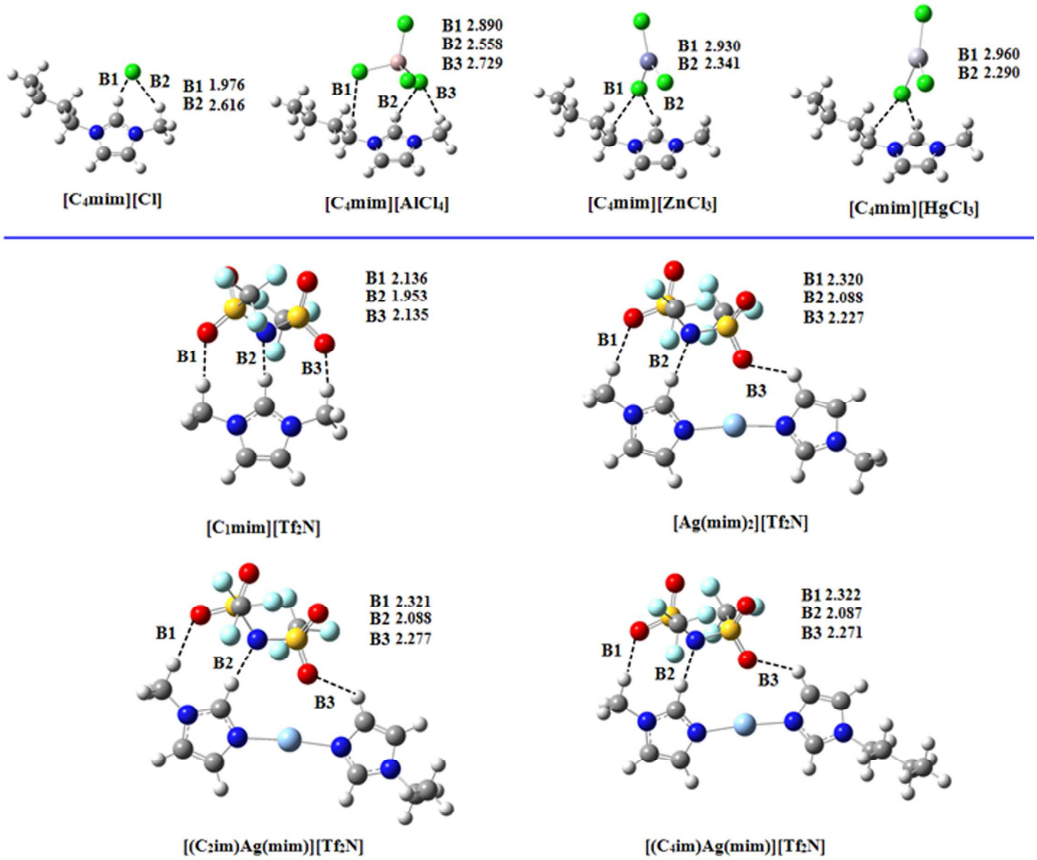

Fig. 1 Optimized structures of the ion pairs for the ILs under study. Distances are in angstroms.

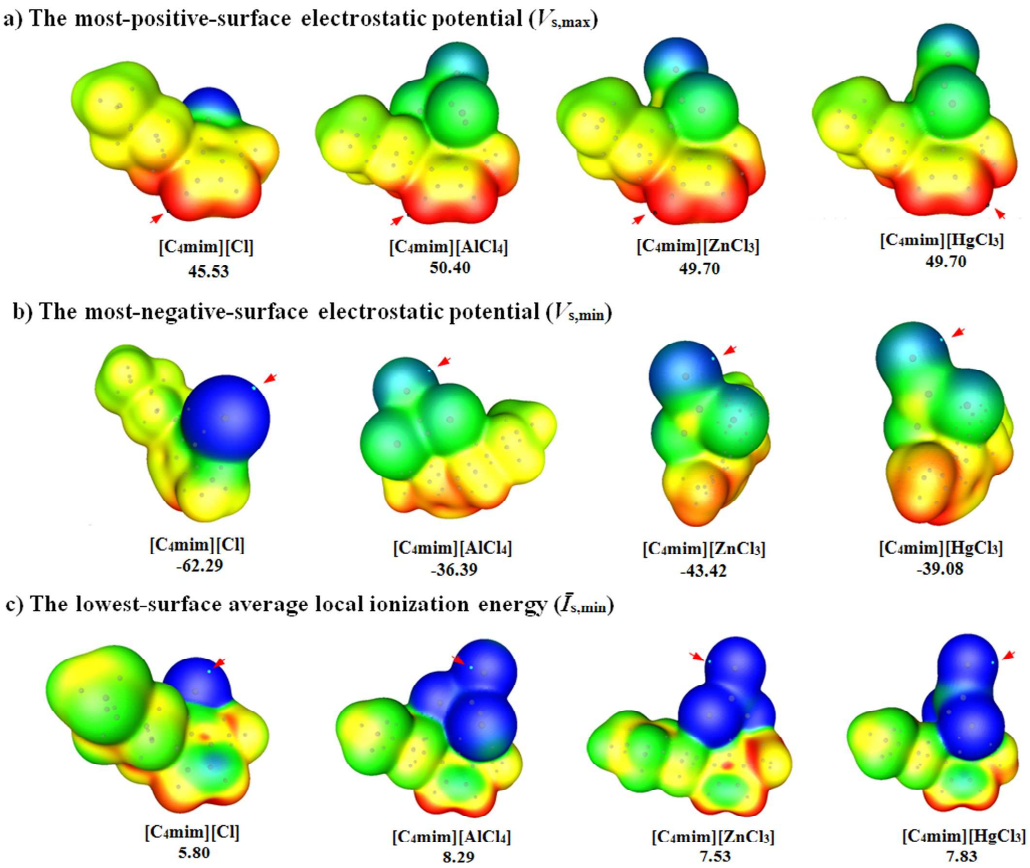

Fig. 2 Molecular surface properties of chlorometallate ILs and [C_4mim][Cl: (a) electrostatic potential at the 0.001 au contour of the electron density and its maximum $V_{s,max}$ on the ILs; (b) electrostatic potential at the 0.001 au contour of the electron density and its minimum $V_{s,min}$ on the ILs; (c) average local ionization energy at the 0.001 au contour of the electron density and its minimum $\bar{I}_{s,min}$ on the ILs. Color ranges for electrostatic potential, in kcal/mol: blue < −30.0 < green < -4 < yellow < 20 < red. Color ranges for average local ionization energy, in eV: blue < 10 < green < 12 < yellow < 14 < red. The positions of $V_{s,m}$ and $\bar{I}_{s,min}$ are marked by the red arrow on the surface.

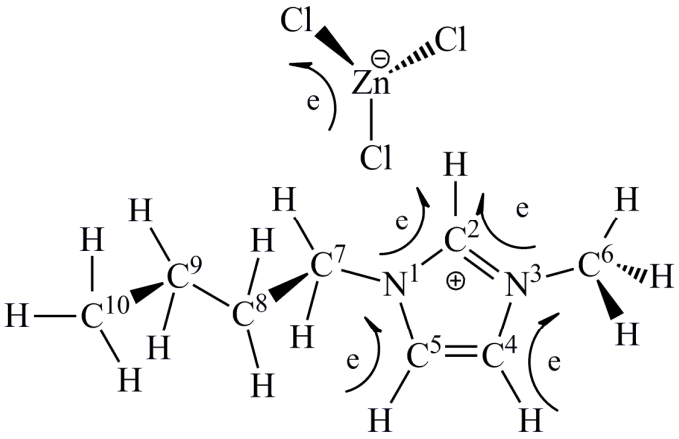

Fig. 3 Direction of charge transfer when $ZnCl_2$ approaches the ion pair unit (C_4mim-Cl).

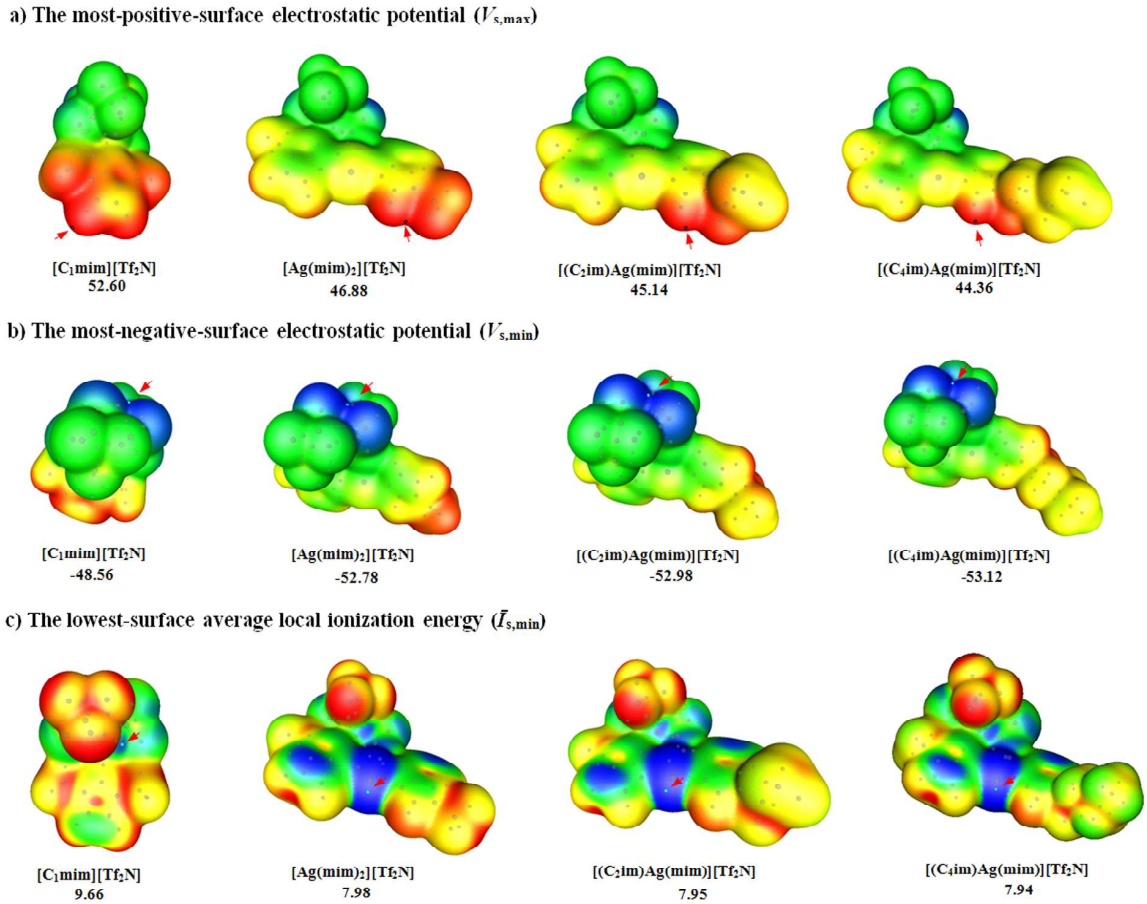

Fig. 4 Molecular surface properties of silver-containing ILs and $[C_1mim][Tf_2N]$,: (a) electrostatic potential at the 0.001 au contour of the electron density and its maximum $V_{s,max}$ on the ILs; (b) electrostatic potential at the 0.001 au contour of the electron density and its minimum $V_{s,min}$ on the ILs; (c) average local ionization energy at the 0.001 au contour of the

electron density and its minimum $\bar{I}_{s,min}$ on the ILs. Color ranges for electrostatic potential, in kcal/mol: blue < −30.0 < green < -4 < yellow < 20 < red. Color ranges for average local ionization energy, in eV: blue < 10 < green < 12 < yellow < 14 < red. The positions of $V_{s,m}$ and $\bar{I}_{s,min}$ are marked by the red arrow on the surface.

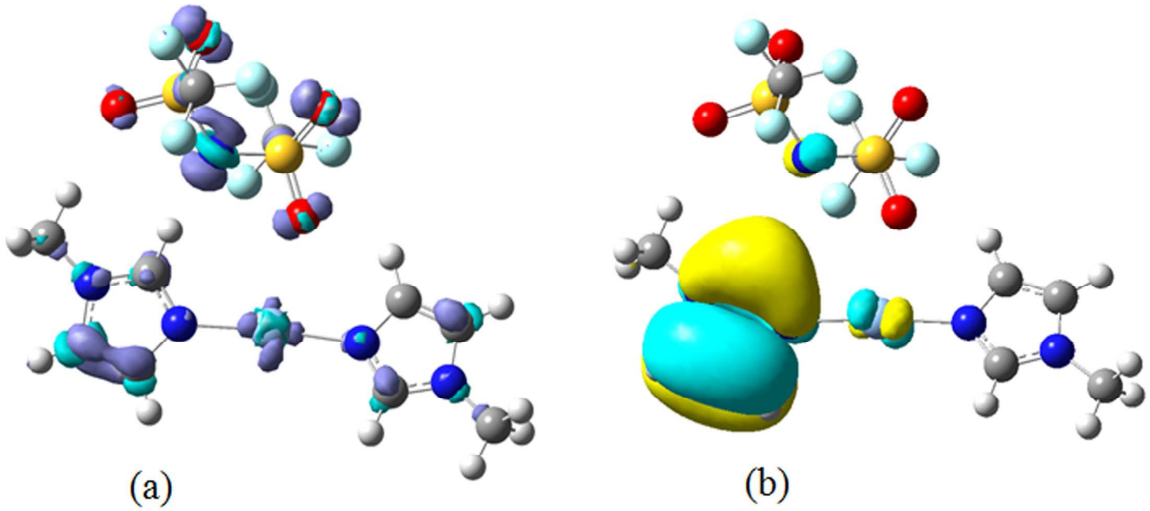

Fig. 5 The electron donor Fukui function f^- isodensity plot at 0.003 a.u. (a) and the HOMO orbital at 0.03 a.u. (b) of $[Ag(min)_2][Tf_2N]$.